

1 **Analysis of the drought recovery of Andosols on southern** 2 **Ecuadorian Andean páramos**

3 **V. Iñiguez**^{1,2,3}, **O. Morales**¹, **F. Cisneros**¹, **W. Bauwens**², **G. Wyseure**³

4 [1]{Programa para el manejo del Agua y del Suelo (PROMAS), Universidad de Cuenca,
5 Cuenca, Ecuador}

6 [2]{Department of Hydrology and Hydraulic Engineering, Earth System Sciences Group,
7 Vrije Universiteit Brussel (VUB), Brussels, Belgium}

8 [3]{Department of Earth and Environmental Science, KU Leuven, Leuven, Belgium}

9

10 Correspondence to: vicente.iniguez@ucuenca.edu.ec

11 **Abstract**

12 The Neotropical Andean grasslands above 3500 m a.s.l. known as páramo offer remarkable
13 ecological services for the Andean region. Most important is the water supply of excellent
14 quality to many cities and villages established in the inter-Andean valleys and along the coast.
15 However, the páramo ecosystem is under constant and increased threat by human activities
16 and climate change. In this paper we study the recovery of its soils for drought periods
17 observed during 2009 and 2012. In addition, field measurements and hydrological conceptual
18 modelling at the catchment-scale are comparing two contrasting catchments in the southern
19 Ecuadorian Andes. Both were intensively monitored in order to analyse the temporal
20 variability of the soil moisture storage. A typical catchment on the páramo at 3500 m a.s.l.
21 was compared to a lower grassland one at 2600 m a.s.l. The main aim was to estimate the
22 severity of the drought periods by means of drought analysis and the recovery during a
23 subsequent wet period. Local soil water content measurements in the top soil (first 30 cm)
24 through TDR (plot scale) were compared to the average soil water storage as estimated by the
25 probabilistic soil moisture (PDM) model (catchment scale) in order to reveals the impact of
26 different scales over the drought analysis. This conceptual hydrological model with 5
27 parameters was calibrated and validated for both catchments. At the plot scale, the study
28 reveals an apparently high recovery of this type of shallow organic soils during the droughts
29 in 2009 and 2010. During these droughts, the soil water content dropped from a normal value

1 of about 0.80 to $\sim 0.60 \text{ cm}^3 \text{ cm}^{-3}$, while the recovery time was two to three months. This did
2 not occur at lower altitudes (Cumbe) where mineral soils needed about eight months to
3 recover from the drought in 2010. The soil moisture depletion observed in the mineral soils
4 was similar to the Andosols (27%), decreasing from a normal value of about 0.54 to ~ 0.39
5 $\text{cm}^3 \text{ cm}^{-3}$, but the recovery was slower. However, at the catchment scale the differences in the
6 recovery are not significant. The precipitation is the main factor in the hydrological response
7 at the catchment scale. Finally, the drought analysis reveals small deficits for the soil
8 moisture droughts in both experimental catchments.

9

10 **1 Introduction**

11 In the northern Andean landscape, between ca. 3500 and 4500 m a.s.l., an “alpine”
12 Neotropical grassland ecosystem -locally known as “páramo”- covers the mountains. Their
13 major ecological characteristics have been documented by several authors (e.g. Buytaert et al.,
14 2006a; Hofstede et al., 2003; Luteyn, 1999). The páramo is an endemic ecosystem with high
15 biodiversity. Its soils contain an important carbon storage and provide a constant source for
16 drinking water for many cities, villages, irrigation systems and hydro-power plants. During
17 the last years, a high vulnerability of these systems to changes induced by human activities
18 and climate change in mountainous regions has been recognized. Most of the research in
19 páramos has been focused on its hydrological capacity as well as the soil characteristics under
20 unaltered and altered conditions (Buytaert et al., 2007a; Farley et al., 2004; Hofstede et al.,
21 2002; Podwojewski et al., 2002). These researches recognize the key role of the páramos in
22 the water supply in the Andean region. The hydrological capacity is mainly related to the
23 characteristics of its soils. Shallow organic soils classified according to the World Reference
24 Base for Soil Resources (WRB) as Andosols and Histosols (FAO et al., 1998) are the two
25 main groups of soils that can be found in this Andean region. In addition, but less frequently,
26 also Umbrisols, Regosols and other soils may be found. These soils are characterized by high
27 levels of organic matter. They have an immense water storage capacity which reduces flood
28 hazards for the downstream areas, while sustaining the low flows all year round for domestic,
29 industrial and environmental uses.

30 In the wet páramos that we investigated –and which have a low seasonal climate variability–
31 the high water production can be explained by the combination of a somewhat higher
32 precipitation and -more importantly- a lower water consumption by the vegetation. In these

1 conditions, the role of the soil water storage capacity would not be significant. This is in
2 contrast with páramos with a more distinct rainfall seasonal variability (as e.g. in the western
3 part of the highlands of the Paute river basin), where the hydrological behaviour of the
4 páramo ecosystem is more influenced by the water holding capacity of the soils (Buytaert et
5 al., 2006a). Rainfall ranges between 1000 and 1500 mm year⁻¹ and is characterized by
6 frequent, low volume events (drizzle) (Buytaert et al., 2007b). The annual runoff can be as
7 high as 67% of the annual rainfall (Buytaert et al., 2006a). During wet periods the volumetric
8 soil water content ranges between 80% and 90%, with a wilting point around 40%. So the soil
9 water holding capacity is high as compared to mineral soils. This is a very important factor in
10 the hydrological behaviour of the páramo. This larger storage is important during dry periods
11 and explains the sustained base flow throughout the year. The soil physical characteristics
12 such as porosity and microporosity –which is much higher than what is commonly found in
13 most soil types– explains an important part of the regulation capacity during dry periods. The
14 water buffering capacity of these ecosystems can also be explained by the topography, as the
15 irregular landscape contains many concavities and local depressions where bogs and small
16 lakes have developed (Buytaert et al., 2006a).

17 Nevertheless, the páramo area is under threat by the advance of the agricultural frontier.
18 Additionally, flawed agricultural practices cause soil degradation and erosion. Former studies
19 on soil water erosion reveal significant soil loss in the highlands of the Ecuadorian Andean as
20 result of land use changes (Vanacker et al., 2007) but also tillage erosion is responsible for
21 this soil loss and for the degradation of the water holding capacity (Buytaert et al., 2005;
22 Dercon et al., 2007).

23 Land cover changes have also occurred in páramo. In the seventies, some areas of páramo
24 were considered appropriate for afforestation with exotic species such as *Pinus radiata* and
25 *Pinus patula*. The main goal was to obtain an economical benefit from this commercial
26 timber. The negative impact of this afforestation and the consequences on the water yield of
27 the páramo have been described by Buytaert et al. (2007b). Also, the productivity was often
28 rather disappointing, due to the altitude.

29 The potential impact of the climate change over alpine ecosystems has also been reported by
30 Buytaert et al., 2011 and Viviroli et al., 2011. Mora et al. (2014) predicted an increase in the
31 mean annual precipitation and temperature in the region that is of interest to our study.
32 Therefore, the carbon storage and the water yield could be reduced by the higher temperatures

1 and the larger climate variability. However, the uncertainties on the potential impact of the
2 climate change remain high (Buytaert and De Bièvre, 2012; Buytaert et al., 2010).

3 Additionally, the occurrence of drought periods in the páramo have a negative impact on the
4 water supply and on the economy of the whole region that depends on water supply from the
5 Andes. For instance, the water levels in the reservoir of the main hydropower project in the
6 Ecuadorian Andes –the Paute Molino project– reached their lowest values as a consequence
7 of the drought between December 2009 and February 2010. This caused several, intermittent,
8 power cuts in many regions of Ecuador. The power plant’s capacity is 1075 MW. In that
9 period the Paute Molino hydropower provided around 60% of Ecuador’s electricity
10 (Southgate and Macke, 1989).

11 It is claimed that the hydrological regulation and buffering capacity is linked to its soils
12 (Buytaert et al., 2007b). Therefore the present study investigates the response of páramo soils
13 to drought and compares with other soils on grasslands at lower altitude in the same region.
14 The drought analysed is a hydrological and soil water drought as defined by Van Loon
15 (2015).

16 The major point in our research is to analysis the recovery speed of the páramo soils after
17 drought periods. Indeed, our hydrological perspective serves -in the first place- the
18 downstream users. The observation period includes the droughts of 2009, 2010, 2011 and
19 2012 together with intermediate wet periods.

20 In this paper hydrological drought is compared and related to soil water drought by analysing
21 the drought propagation. Two experimental catchments –one with and one without páramo–
22 were investigated. The results from the hydrological model and drought analysis in terms of
23 soil water storage were compared. In the two catchments rainfall, climate, flow and soil
24 moisture by TDR in experimental plots was measured. A parsimonious conceptual
25 hydrological model –using The Probability Distributed Moisture simulator (PDM), a
26 parsimonious conceptual hydrological model, was calibrated and validated for each
27 experimental catchment. The PDM model allowed to analyse the temporal and spatial
28 variability of the soil water content as well as the maximum storage capacity at the catchment
29 scale.

30 In this context, the hydrological model (PDM) used in the research tried to link soil moisture
31 storage (as indicator for soil water drought) with the stream discharge (as indicator for the
32 hydrological drought).

1

2 **2 Materials**

3 **2.1 Study area**

4 The catchments under study are located in the southwest highlands of the Paute river basin,
5 which drains to the Amazon River (Fig. 1). These highlands form part of the Western
6 Cordillera in the Ecuadorian Andes with a maximum altitude of 4420 m a.s.l. The study area
7 comprises a mountain range from 2647 until 3882 m a.s.l. Two catchments have been selected
8 from this region: Calluancay and Cumbe.

9 The Calluancay catchment has an area of 4.39 km² with an altitude range between 3589 and
10 3882 m a.s.l. and a homogeneous páramo cover. The páramo vegetation consists mainly of
11 tussock or bunch grasses and very few trees of the genus *Polylepis*. These trees are observed
12 in patches sheltered from the strong winds by rock cliffs or along to some river banks in the
13 valleys. Furthermore, in saturated areas or wetlands huge cushion plants are surrounded by
14 mosses. This vegetation is adapted to extreme weather conditions such as low temperatures at
15 night, intense ultra-violet radiation, the drying effect of strong winds and frequent fires
16 (Luteyn, 1999). The land use of Calluancay is characterized by extensive livestock grazing.

17 The second catchment, Cumbe, drains an area of 44 km². The highest altitude reaches 3467 m
18 a.s.l., whereas the outlet is at an altitude of 2647 m. This altitude range of almost 1000 m
19 defines a typical Andean mountain landscape with steep slopes and narrow valleys where the
20 human intervention is also evident. This catchment is below the 3500 m and therefore
21 contains a negligible area of páramo. The most prominent land cover is grassland (38.1%)
22 along with arable land and rural residential areas (26.9%). A sharp division between the
23 residential areas and the small scale fields is absent. Mountain forest remnants are scattered
24 and cover 23% of the area, often on the steeper slopes. At the highest altitude (>3300 m) sub-
25 páramo is predominant; it occupies only 7.6% of the catchment. In the Cumbe catchment,
26 about 4.4% of the area is degraded by landslides and erosion.

27 A small village, “Cumbe”, is located in the valley and on the lower altitudes of the catchment.
28 This village has ca. 5550 inhabitants. The water diversions from streams in Cumbe are ca. 12
29 [L s⁻¹] in total, mainly for drinking water. The village has no waste water treatment and used
30 water is discharged via septic tanks. Additionally, during dry periods two main open water
31 channels for surface irrigation are enabled. The water diversion and its rudimentary hydraulic

1 structures have been built upstream of the outlet of the catchment. These irrigation systems
2 deliver water to the valley area occupied by grasslands and small fields with crops.

3 Several types of soils can be identified in Cumbe and Calluancay, which are mainly
4 conditioned by the topography. Dercon et al. (1998, 2007) have described the more common
5 toposequences in the southern Ecuadorian Andes according to the WRB classification (FAO
6 et al., 1998). Cumbe has a toposequence of soils from Vertic Cambisols, located in the
7 alluvial area, surrounded by Dystric Cambisols at the hillslopes in the lower and middle part
8 of the catchment. Eutric Cambisols or Humic Umbrisols extend underneath the forest patches
9 between 3000 and 3300 m a.s.l. The highest part of the catchment -from 3330 until 3467 m
10 a.s.l.- is covered by Humic Umbrisols or Andosols.

11 In contrast, Calluancay is characterized by two groups of organic soils under páramo:
12 Andosols (in the higher and steeper parts) and Histosols (in the lower and gentler parts of the
13 catchment). The soils were formed from igneous rocks such as andesitic lava and pyroclastic
14 igneous rock (mainly the Quimsacocha and Tarqui formations, dating from the Miocene and
15 Pleistocene respectively), forming an impermeable bedrock underneath the catchment. In the
16 Cumbe catchment, the highlands and some areas of the middle part (about 55% of the area)
17 are characterized by pyroclastic igneous rocks (mainly the Tarqui formation). The valley area
18 (37% of the basin) is covered by sedimentary rocks like mudstones and sandstones (mainly
19 the Yunguilla formation, dating from the upper Cretaceous). Only 8% of the Cumbe
20 catchment comprises alluvial and colluvial deposits, which date from the Holocene
21 (Hungerbühler et al., 2002).

22

23 **2.2 Monitoring of hydro-meteorological data**

24 An intensive monitoring with a high time resolution was carried out in the study area during
25 28 months.

26 The gauging station at the outlet of Cumbe consists of a concrete trapezoidal supercritical-
27 flow flume (Kilpatrick and Schneider, 1983) and a water level sensor (WL16 - Global Water).
28 Logging occurs at a 15 minute time interval. Regular field measurements of the discharge
29 were carried out to cross-check the rating curve. Initially a smaller catchment, similar in size
30 to the Calluancay, was also equipped within the Cumbe catchment but a landslide destroyed
31 and covered this flume. So, unfortunately no data were collected.

1 The measurements at Calluancay were part of a larger hydrological monitoring network
2 maintained by PROMAS. Water levels were logged every 15 minutes at two gauging stations,
3 which consist of a concrete V-shaped weir with sharp metal edges and a water level sensor
4 (WL16- Global Water). The first station was installed at the outlet of the catchment. The
5 second gauging station monitors an irrigation canal to which water is diverted from the main
6 river. The gauging station was installed where the canal passes the water divide of the
7 catchment. So, the total discharge can be evaluated.

8 For the Calluancay, rainfall is measured by a tipping bucket rain gauge (RG3M-Onset HOBO
9 Data Loggers) located inside the catchment and with a resolution of 0.2 mm.

10 Three similar rain gauges were installed in the larger Cumbe catchment and located at the
11 high, middle and lower part of the catchment. The areal rainfall for Cumbe was calculated
12 with the inverse distance weighing (IDW) method, using the R implementation of GSTAT
13 (Pebesma, 2004).

14 In each experimental catchment the meteorological variables such as air temperature, relative
15 humidity, solar radiation and wind speed were measured with a 15 minute time interval by an
16 automatic weather station. These stations were used to estimate the potential reference
17 evapotranspiration according to the FAO-Penman-Monteith equation.

18

19 **2.3 Measurement of soil water content**

20 In both catchments, the soil moisture content of the top soil layer was measured by means of
21 time domain reflectometry (TDR) probes at representative sites in the vicinity of the weather
22 stations. In each catchment there was one plot equipped with 6 TDR's with a data-logger.

23 As TDR-sensors with data-logger per plot require a very large investment, the locations for
24 the TDR measurements were carefully selected based on a digital terrain analysis, the soil and
25 land cover maps and field surveys (soil profile pits). In Calluancay, the soil information was
26 available from former studies by PROMAS between 2007 and 2009. In this period, a soil map
27 (scale 1:10 000) -which covered the whole altitudinal range of páramo (3500-3882 m a.s.l.)-
28 was generated based on soil descriptions of 2095 vertical boreholes and 12 soil profile pits.
29 For each soil profile pit a physico-chemical analysis of each layer were executed. Within the
30 Cumbe catchment 13 soil profile pits were dug as part of the present research. Thus, for both
31 catchments a detailed soil map was available covering the whole altitudinal range (2647 –

1 3882 m a.s.l.). Based on this detailed soil information representative locations for the TDR
2 measurements in each catchment were selected.

3 The TDRs were installed vertically from the soil surface with a length of 30 cm and logged at
4 15 minute time intervals. In Calluancay, every fortnight soil water content was also measured
5 by sampling from November 2007 until November 2008. In this catchment the TDR time
6 series was from May 2009 until November 2012. In Cumbe, the TDR-time series extends
7 from July 2010 until November 2012.

8 For Cumbe and Calluancay, the TDR probes were calibrated based on gravimetric
9 measurements of soil moisture content, using undisturbed soil samples ($r^2 = 0.79$ and 0.80
10 respectively). In addition, the curves were regularly cross-validated by undisturbed soil
11 samples during the monitoring period.

12 The soil water retention curves were determined based on undisturbed and disturbed soil
13 samples collected near to the TDR probes. In the laboratory, pressure chambers in
14 combination with a multi-step approach allowed to define pairs of values for moisture (θ) and
15 matric potential (h). The soil water retention curve model proposed by van Genuchten (1980)
16 was fitted on the data.

17

18 **3 Methods**

19 **3.1 Catchment modelling**

20 The hydrological PDM model (Moore and Clarke, 1981; Moore, 1985) is a conceptual rainfall
21 – runoff model, which consists of two modules. The first one is the soil moisture accounting
22 (SMA) module which is based on a distribution of soil moisture storages with different
23 capacities accounting for the spatial heterogeneity in a catchment. The probability distribution
24 used is the Pareto distribution. The SMA module simulates the temporal variation of the
25 average soil water storage. The second part of the model structure is the routing module,
26 which consists of two linear reservoirs in parallel in order to model the fast and slow flow
27 pathways, respectively.

28 Based on geological data, in Calluancay the deep percolation and capillary rise fluxes are
29 considered to be negligible since the soils overlay bedrock consisting of igneous rocks with
30 limited permeability. In páramos, saturation overland flow is the dominant flow process of
31 fast runoff generation (Buytaert and Beven, 2011). Lateral subsurface flow has a slower

1 response. Therefore, the stream discharge at the outlet of the catchment thus comprises
2 mainly fast overland flow and slow lateral flow.

3 In Cumbe, a surface-based electrical resistivity tomography test (Koch et al., 2009; Romano,
4 2014; Schneider et al., 2011) of a cross-section revealed no significant shallow groundwater
5 for the alluvial area. In addition, the flat alluvial area surrounding the river near the catchment
6 outlet is very small (2.7 % of the catchment area). Therefore, deep percolation and capillary
7 rise are also regarded to be negligible.

8 As clay is the most important soil texture in Cumbe it is inferred that the infiltration overland
9 flow is the dominant flow process of runoff generation. As a result, the stream discharge in
10 Cumbe consists, as in Calluancay, by the combination of overland either due to limited
11 infiltration or to saturation and of shallow lateral flow.

12 The PDM model was implemented within a MATLAB toolbox using the options of
13 calculating the actual evapotranspiration E_a as a function of the potential evaporation rate E_p ,
14 and the soil moisture deficit by (Wagener et al., 2001):

15

$$16 \quad E_a = \left\{ 1 - \left[\frac{(S_{max} - S(t))}{S_{max}} \right] \right\} \cdot E_p \quad (1)$$

17

18 Where, S_{max} is the maximum storage and $S(t)$ is the actual storage at the beginning of the
19 interval. A description of the model parameters is provided in Table 2.

20 The actual evapotranspiration estimated by PDM model as compared to the potential
21 vegetation evapotranspiration is an indicator of the drought stress.

22 **3.1.1 The potential evapotranspiration**

23 The FAO-Penman-Monteith approach (Allen et al., 1998) was used to estimate the potential
24 evapotranspiration of a reference crop (similar to short grass) under stress free conditions
25 without water limitation:

26

$$27 \quad E_p = \frac{0.408\Delta(R_n - G_h) + \gamma \frac{900}{T + 273} u_2 (e_s - e_a)}{\Delta + \gamma(1 + 0.34u_2)} \quad (2)$$

1

2 Where:

3 E_p = the potential reference evapotranspiration [mm day^{-1}],

4 R_n = the net radiation at the crop surface [$\text{MJ m}^{-2} \text{day}^{-1}$],

5 G_h = the soil heat flux density [$\text{MJ m}^{-2} \text{day}^{-1}$],

6 T = the mean daily air temperature at 2 m height [$^{\circ}\text{C}$],

7 u_2 = the wind speed at 2 m height [m s^{-1}],

8 e_s = the saturation vapour pressure [kPa],

9 e_a = the actual vapour pressure [kPa],

10 $e_s - e_a$ = the saturation vapour pressure deficit [kPa],

11 Δ = the slope of the vapour pressure curve [$\text{kPa } ^{\circ}\text{C}^{-1}$],

12 γ = the psychrometric constant [$\text{kPa } ^{\circ}\text{C}^{-1}$].

13

14 The suitability of the FAO-Penman-Monteith approach for high altitudinal areas has been
15 evaluated by Garcia et al. (2004). They found that the FAO-approach gives the smallest bias
16 (-0.2 mm day^{-1}) as compared to lysimetric measurements.

17 The measurements of the solar radiation by the meteorological stations in our experimental
18 catchments were not consistent and considered to be unreliable. Therefore the solar radiation
19 was estimated by the Hargreaves-Samani equation (Hargreaves and Samani, 1985) using the
20 daily maximum and minimum air temperature:

21

$$22 \quad R_s = R_a c (T_{\max} - T_{\min})^{0.5} \quad (3)$$

23

24 Where:

25 R_s = the solar radiation [$\text{MJ m}^{-2} \text{day}^{-1}$],

26 R_a = the extra-terrestrial solar radiation [$\text{MJ m}^{-2} \text{day}^{-1}$],

27 c = an empirical coefficient [-],

1 T_{\max}, T_{\min} = the daily maximum and minimum air temperature respectively [°C],
2 According to Hargreaves and Samani (1985) “ c ” has a value of 0.17 for inland areas.
3

4 **3.1.2 The actual evapotranspiration**

5 The potential evapotranspiration of a vegetation without drought stress can be calculated by
6 multiplying the reference crop evapotranspiration by a vegetation coefficient k_v . During dry
7 periods, with water stress, the vegetation extracts less water as compared to the vegetation
8 requirement. The relative reduction of the evapotranspiration due to this may be expressed by
9 a water stress coefficient k_s . During stress free periods k_s equals to one and the lower the stress
10 coefficient the more stress the vegetation experiences.

11 The actual evapotranspiration, E_a , can thus be calculated as:

$$13 \quad E_a = k_s \cdot k_v \cdot E_p \quad (4)$$

14

15 In general, k_v is time-dependent, as it is linked to the growth cycle of the vegetation and thus
16 to the season. For páramo close to the equator, this seasonality may be neglected as the
17 grasses are slow-growing and perennial.

18 For the purpose of this study the global effect of both coefficients will be estimated and the
19 Eq. (4) can be combined into one coefficient K :

20

$$21 \quad E_a = K \cdot E_p \quad (5)$$

22

23 In order to determine K the actual and potential evapotranspiration need to be estimated.

24 **3.1.3 Calibration and validation of PDM model**

25 A split sample test is performed in order to assess the performance of the PDM model and so,
26 calibration and validation periods are established (Klemeš, 1986). The collected data contain
27 wet and dry periods.

1 To implement the PDM model, an exploratory sensitivity analysis was done in order to define
2 the feasible parameter range. The sampling strategy applied was an optimal Latin Hypercube
3 sampling with a genetic algorithm according to (Stocki, 2005) and (Liefvendahl and Stocki,
4 2006). Afterwards, the obtained parameters of the PDM model were optimized by means of
5 the Shuffled Complex Evolution algorithm (Duan et al., 1992).

6 The time periods from 29 November 2007 until 06 August 2009 and from 20 May 2010 until
7 27 November 2012 were used as calibration and validation period respectively for
8 Calluancay. In the case of Cumbe, the calibration and validation periods were respectively
9 from 21 April 2009 until 17 April 2011 and from 18 April 2011 until 13 December 2012. The
10 selected periods for calibration and validation contained the typical climatic conditions of the
11 southern Ecuadorian Andes (Buytaert et al., 2006b; Celleri et al., 2007).

12 The Nash and Sutcliffe efficiency (NSE) was used as objective function (Nash and Sutcliffe,
13 1970) for calibration. As low flows under drought were important the logarithmic discharges
14 were used for the calculation of the NSE.

15 It is important to mention that the measured soil moisture data are not used as input variables
16 to the model. However, as most hydrological models the PDM model generates internally
17 state and output variables. These internally calculated variables include effective rainfall,
18 actual evapotranspiration, simulated discharge and average distribution characteristics of the
19 soil moisture storage. After calibration/validation of the parameters the simulated PDM
20 average soil water content was compared to the observed soil water content, measured by
21 TDR in one experimental plot in each catchment. The average soil water content simulated by
22 PDM was used in the drought analysis.

23 In the PDM, there is no explicit modelling of soil surface evaporation, and therefore it cannot
24 estimate the soil water storage below the wilting point. The soil water content always
25 remained higher than wilting point. The volumetric water storage at wilting point, which is in
26 Andosols and Histosols still as high as 40%, was therefore not actively represented in the
27 model and can be considered as dead storage from the PDM modelling point of view.

28

29 **3.2 Drought analysis**

30 The severity of drought periods were identified and quantified by a threshold level approach
31 (Andreadis et al., 2005; Van Lanen et al., 2013; Van Loon et al., 2014). Thresholds were set

1 for the time series of precipitation (P), observed stream discharge (Q) and average soil water
2 content simulated by PDM (S) according to Van Loon et al., (2014):

3 - a threshold for each month of the year was based on the 80th percentile of duration curves of
4 P , S and Q applying a 10 day moving average. This threshold was subsequently smoothed by
5 a 30 day moving average. Last smoothing removed the stepwise pattern and avoided artefact
6 droughts at the beginning or end of a month (Van Loon, 2013).

7 -Drought characteristics are determined based on a deficit index:

8

$$9 \quad d(t) = \begin{cases} \tau(t) - x(t) & \text{if } x(t) < \tau(t) \\ 0 & \text{or} \\ & \text{if } x(t) \geq \tau(t) \end{cases} \quad (6)$$

10

11 Where, $x(t)$ is the hydrometeorological variable on time t and $\tau(t)$ is the threshold level of the
12 hydrological variable on time t . The units are mm day⁻¹ and time t is measured in days. The
13 deficit of drought event i (D_i) is then given by

14

$$15 \quad D_i = \sum_{t=1}^T d(t) \cdot \Delta t \quad (7)$$

16

17 in which D_i is in mm. The deficit is standardized by dividing by the mean of the
18 hydrometeorological variable $x(t)$. A physical interpretation of standardized deficit is the
19 number of days with mean flow required to reduce the deficit to zero (Van Loon et al., 2014).

20

21 **3.2.1 Drought propagation and drought recovery analysis**

22 Here, we analysed the translation -as a chain of hydrological processes- from meteorological
23 drought over soil water drought into hydrological drought for the catchment. The time series
24 of P , Q and S was in one figure per catchment. This allowed a visual inspection of the
25 propagation, onset and recovery of droughts and to compare the behaviour of the different
26 time series.

1 The Fig. 2 shows a conceptual graph for the estimation of the drought recovery. This diagram
2 is similar to the formulated by Parry et al., (2016), who have proposed an approach to
3 systematic assessment of the drought recovery period or drought termination. Such graphs
4 allow to determine the duration t_d in days of a drought. The drought starts when the variable
5 drops under the threshold and ends when the normal state is reached again. The duration of
6 drought recovery, t_{dr} , starts from the lowest point to the end of drought. The slope of the
7 variable between the lowest point and the end estimates the rate of recovery. This rate can be
8 expressed as percentage of the recovery per day with respect to the normal value for the
9 variable.

10

11 **3.2.2 Vegetation stress and recovery**

12 Drought indices have been used by several researchers in order to quantify drought
13 characteristics (Dai, 2011; Van Loon, 2015; Tsakiris et al., 2013). Most of them are based on
14 Precipitation P and potential evapotranspiration E_p . For instance, the Standardized
15 Precipitation Index (SPI) (Lloyd-Hughes and Saunders, 2002) or the Standardized
16 Precipitation and Evapotranspiration Index (SPEI) (Vicente-Serrano et al., 2013) are widely
17 used in drought studies. But, due to the lack of a long historical time series of climate data for
18 our experimental area, this type of indices cannot be applied. Nevertheless, based on the
19 available monthly time series of P and E_p a comparison can be done between catchments.

20 For this purpose, month have potentially water shortage for the vegetation when the potential
21 evapotranspiration exceeds the rainfall:

22
$$E_p > P \tag{8}$$

23 And, a stress period is defined as result of the total sum of consecutive months where
24 vegetation stress is identified. Modelling by PDM was used to estimate E_a and was compared
25 with the E_p .

26 After the stress periods, when the wet season starts P reaches values to cover the deficit of
27 soil water and the vegetation starts to recover. These periods are also identified based on the
28 monthly data of P and E_p and contrasted with E_a estimations. When E_a reaches the highest
29 value -normally during the wet season- that month marks the end of the vegetation recovery.

30

3.2.3 Sensitivity analysis

A sensitivity analysis was carried out by the PDM model in order to reveal the most important factor in the recovery of the soils after drought periods. The factors are climate -precipitation and potential evapotranspiration- and soils.

The parameters set obtained during the calibration procedure -which basically reassembles the soil water storage characteristics for each catchment- is the first factor S . The second and third factors are precipitation P and potential evapotranspiration E_p . Two scenarios were regarded:

1) For Calluancay, the parameters which defined the S were not modified in the model but P and E_p based on meteorological data in Cumbe were used as input data in order to assess the impact on S . The same scenario was applied to Cumbe, the S defined by the parameters set calibrated were not modified but P and E_p registered in Calluancay were regarded as input data to the model of Cumbe.

2) The S and P in both catchments were not modified but the E_p was exchanged.

The scenario results, simulated stream discharge Q_{sim} and average soil water storage S are displayed in plots for each catchment in order to establish the main differences. Positive or negative deviations from the original simulation (calibration) will reveal the impact of the climate over the soil water storage and stream discharge. The analysis of the scenario results is focus in the drought recovery periods in order to compare the behaviour of the soils during different climate conditions.

4 Results and discussion

4.1 Potential evapotranspiration

The potential reference evapotranspiration (E_p) for the period from 16 July 2010 until 15 November 2012 was calculated by the FAO-Penman-Monteith approach with the solar radiation estimated by Hargreaves-Samani. The daily average of E_p for Calluancay and Cumbe was 2.35 and 3.04 mm day⁻¹ respectively. The temporal variation of E_p is depicted in Fig. 3. It reveals a sinusoidal pattern with higher atmospheric evaporative demand during the drier months (from August to March) and a lesser demand during the subsequent wet periods (from April to July). E_p ranged between 0.76 and 4.17 mm day⁻¹ for Calluancay and between 1.56 and 4.62 mm day⁻¹ for Cumbe. The difference can be attributed to the altitude difference

1 between both catchments, with 900 m difference in elevation. The daily average minimum
2 and maximum temperatures in Calluancay were 3.0 and 10.2 °C respectively, while, in
3 Cumbe they were 7.8 and 17.4 °C. In addition, the wind speed is different in both catchments.
4 Calluancay is very exposed to prevailing winds while Cumbe is relatively sheltered. The daily
5 average wind speed for Calluancay and Cumbe was 4.2 (max: 11.9) and 0.9 (max: 2.6) m s⁻¹
6 respectively.

7 **4.2 Modelling the discharge and the actual evapotranspiration**

8 The Table 3 and Fig. 4 summarizes the results for the PDM model. The performance of the
9 model for the calibration period is good in both catchments (Nash-Sutcliffe efficiency, NSE=
10 0.83). Lower values of NSE were obtained during the validation periods. The calibration
11 focussed on low flows. More storm runoff events were observed during the validation period
12 as a consequence the poorer fit of large flows led to lower NSE.

13 The average soil moisture storage simulated by the PDM model was compared to the
14 observed soil moisture measurements on representative plots (Fig. 4). Similar dynamics are
15 observed. However a more precise up-scaling (from plot to catchment) would benefit from
16 more plots per catchment.

17 Table 2 shows the calibrated parameter set for both catchments. The maximum storage
18 capacity c_{\max} is as expected higher at Calluancay. The parameter “b” is quite different
19 between the 2 catchments. This difference of “b” can be partially attributed to the fact that
20 Cumbe is much larger and less homogeneous and therefore the variety of soils is larger which
21 was reflected in the coefficient representing the variability of soil water storage capacity. The
22 residence time for fast routing is very similar as expected with relatively small catchments.
23 The residence time for slow routing is more different. We know according to recent research
24 by Guzmán et al. (2016) that runoff from hillslopes in the Cumbe catchment infiltrates into
25 the alluvial aquifer, which drains into the river and causes a slow reaction. Calluancay also
26 showed somewhat more contribution of fast flow. This can be explained by the occurrence of
27 saturated overland flow originating from the bogs and wetland parts of the páramo.

28 The daily average values of E_a , as estimated by the PDM model for Calluancay and Cumbe,
29 was 1.47 (range 0.19 to 3.33) and 1.70 (range 0.18 to 3.58) mm day⁻¹ respectively. The PDM
30 model, however, does not regard a critical soil moisture value for vegetation stress and

1 therefore there are no constraints on the evapotranspiration during dry periods. As a result, E_a
2 is overestimated by the model during these events.

3 The impact of both -the vegetation and stress coefficients- globally represented by K
4 coefficient was determined by means of a comparison between E_a and E_p . For Calluancay and
5 Cumbe, the impact of the aforementioned coefficient over the E_a is in average 0.67 (range
6 0.09 to 1.00) and 0.58 (range 0.06 to 1.00) respectively. Buytaert et al. (2006c) determined
7 two values of K for natural and altered páramo vegetation during a period without soil water
8 deficit (k_s equal to 1), 0.42 and 0.58 respectively. Meaning that, if a comparison is done, the
9 average value of K for páramo is higher than the previous research, a 60 and 16%
10 respectively. While, the K value for Cumbe is in line with the literature for grasslands (Allen
11 et al., 1998).

12 Other important fact is that our soil water measurements never reached the wilting point;
13 which is 0.43 and 0.30 $\text{cm}^3 \text{cm}^{-3}$ for Andosols (Calluancay) and Dystric Cambisols (Cumbe),
14 respectively (Fig.4 and Fig. S2 for the water retention curves in supplementary material). The
15 minimum soil water content values during the drought periods in páramo was not lower than
16 0.62 $\text{cm}^3 \text{cm}^{-3}$.

17 The average daily actual evapotranspiration rate of 1.47 and 1.70 mm day^{-1} corresponds with
18 former studies in páramo and grasslands respectively (Allen et al., 1998; Buytaert et al.,
19 2006a). With the E_a estimated, the K coefficients were calculated in order to assess the
20 combined effect of the vegetation and soil water stress. The differences between the
21 catchment is no more than a 16% when average values are compared. Those values were of
22 0.67 and 0.58 for páramo vegetation and grasslands respectively.

23 The relatively low values of K coefficients could be partially explained by the plant
24 physiology. The tussock grasses (mainly *Calamagrostis* spp. and *Stipa* spp.) in páramo are
25 characterized by specific adaptations to extreme conditions. The plants have scleromorphic
26 leaves which are essential to resist intense solar radiation (Ramsay and Oxley, 1997). In
27 addition, the plants are surrounded by dead leaves that protect the plant and reduce the water
28 uptake. In other words, the combination of the xerophytic properties and other adaptations to
29 a high-radiation environment together with the dead leaves lead to a lower water demand as
30 compared to the reference crop evapotranspiration. In Cumbe the grazing pastures are
31 characterized by plants of type C3 (*Pennisetum clandestinum*) which are also highly tolerant
32 to drought. Therefore, the water uptake is mainly regulated by the plants during dry periods.

1 This is clearly observed in the volumetric water content θ as measured by TDR (Fig. 4). Field
2 observations in November 2009, revealed that the plants showed some visual signs of
3 deterioration in the first centimetres but after removal of the top layer, which is always
4 containing dead leaves, the plants itself showed little visual deterioration. Nevertheless, the
5 depletion of the soil moisture storage during dry weather conditions clearly lead to stress and
6 reduced the transpiration rate. As this vegetation has specific adaptations to high-radiation
7 and cold environment the recovery by the vegetation after drought is good. We also think that
8 tillage, burning and artificial drainage might have a larger and more irreversible impact on the
9 soil water holding capacity of the Andosol as compared to this "natural" drought.

10 **4.3 Drought severity**

11 Despite of the soil moisture measurements correspond to a plot-scale still gives a good
12 indication of the severity of the drought periods (Fig. 4). During the drought events in 2009
13 and 2010, the soil water content in páramo dropped substantially. Thus, it was possible to
14 establish the amount of water of the topsoil which is available during these dry periods. The
15 reservoir can deliver a water volume equivalent to $0.24 \text{ cm}^3 \text{ cm}^{-3}$ (this represents the
16 maximum soil water content change) during extreme climate conditions such as the droughts
17 in 2009 and 2010. In normal conditions the maximum change observed in the soil water
18 content in páramo is no more than $0.05 \text{ cm}^3 \text{ cm}^{-3}$.

19 In order to characterize the drought events at catchment scale, a standardized deficit as well as
20 its duration were calculated for each catchment. The results are shown in the figure 5. From
21 this figure is clear to see that the deficit is no more than 9 days for both catchments. In other
22 words, 9 days with mean flow are required to reduce the deficit to zero for the whole set of
23 events. In addition, the duration of the drought events is relatively similar for both catchments
24 with only few outliers as for the case of Cumbe. So, seemingly the drought events
25 characteristics are similar and independent of the climate. This in line with the literature. For
26 instance, based on a global map of Köppen-Geiger climate types (Wanders et al., 2010) and
27 using a similarity index SI (Kim et al., 2003), Van Lanen et al.(2013) concluded that
28 independent of the climate type, similar combinations of duration and standardized deficit
29 volume were found in a large number of drought events. They analysed 1495 locations around
30 the world and a data set over the period 1958 to 2001.

1 This result is confirmed by the values of the slopes of the linear regression models, significant
2 differences are not observed by means of the figure 5. Just a slight higher value of slope for
3 soil water storage in Calluancay (páramo) as compared with Cumbe (grassland) is revealed in
4 this figure. However, it is important to mention that the values of slopes reflect the effect of
5 the drought propagation through the hydrological cycle. A reduced increase of deficit with
6 duration is observed in both catchments. In addition, in Calluancay the standardized deficit
7 and duration in soil water storage are highly correlated. While, in Cumbe, a high correlation is
8 observed in precipitation. In lesser extent, a correlation is observed in discharge for both
9 catchments. The occurrence of hydrological drought events decreased due to high buffering
10 capacity of the soils. This can explain the lack of a high correlation of the standardized deficit
11 and duration in discharge, which has been widely documented in other studies (Van Loon et
12 al., 2014; Peters et al., 2006).

13 **4.4 Drought propagation**

14 The figure 6 shows the drought propagation plots for Calluancay and Cumbe. This figure
15 confirmed the results about the standardized deficit and duration for each drought event as
16 well as the seasonality observed during the monitoring period. The data set is over the period
17 2009 to 2012. A series of relatively consecutive drought periods are observed in the time
18 series of precipitation, which were recorded during the dry season. The dry season normally
19 occurs between August and November and the wet season are concentrated between February
20 and June (Buytaert et al., 2006b; Celleri et al., 2007). And, between August 2009 and March
21 2010 a drought period was observed due to lower precipitation. This event had the longest
22 episode with low rainfall during the whole time series. The soil water storage in both
23 catchments had a crucial role in the propagation of the droughts. For instance, in Cumbe the
24 meteorological drought event of 2009-2010 was almost completely buffered by the soil water
25 storage and hence, the hydrological drought was delayed. The opposite occurred in
26 Calluancay, where the soil water storage at that time was not sufficient to overcome the
27 period with low precipitation. The propagation of the drought was also observed
28 simultaneously in the stream discharge (the hydrological drought). A different pattern is
29 observed between 2010 and 2012. The buffering capacity of soils in Calluancay was higher as
30 compared to Cumbe, since a reduced number of hydrological drought events were observed
31 during that period in Calluancay. The recovery of the soil water storage occurs during the wet

1 season and was caused by several but intermittent storm events, which led to an irregular
2 pattern of the soil water storage.

3 **4.5 Soil water drought recovery**

4 For the 2009-2010 drought event observed in Fig. 6, the duration of the soil water drought
5 recovery for Calluancay and Cumbe was equal to 126 and 176 days respectively. While, the
6 meteorological drought durations were equals to 182 and 238 days respectively. The
7 anomalies calculated were of -59% in Calluancay and -66% in Cumbe.

8 The soil water storage in both catchments decreased up to about 3 mm at the beginning of the
9 drought recovery. The speed of recovery expressed as percentage per day (which is the
10 difference in soil water storage values between the end of drought and the beginning of the
11 drought recovery by divided by the time in days) was of 0.73 and 0.53 % recovery day⁻¹ for
12 Calluancay and Cumbe respectively. This means that, the soil water recovery in Calluancay
13 was a 37% faster as compared to Cumbe. The climate pattern observed for this event
14 explained partially the differences between the rates of recovery. A higher evaporative
15 demand was observed in Cumbe as well as less rainfall. Dividing the precipitation amount by
16 the duration of the drought recovery for each catchment, the differences between the
17 catchments became around 10%. The ratio between P and E_p in Calluancay was 50% higher
18 than in Cumbe. For Calluancay and Cumbe, the soil water droughts started in August and July
19 respectively. These months correspond to the dry season (July – November).

20 For the 2010-2011 soil water drought event, the drought recovery durations for Calluancay
21 and Cumbe were 88 and 90 days respectively. The anomalies were of -61% (Calluancay) and
22 -38% (Cumbe). The speed of recovery was relatively similar in both catchments despite of the
23 differences in the anomalies. The recovery rates were equals to 1.02 (Calluancay) and 0.94 %
24 recovery day⁻¹ (Cumbe). This was almost identical. In this drought event, E_p was significant
25 less than P , as compared with the first drought event. This meant more available water and
26 less deficit. This fact and the difference in the anomalies can explain the similar recovery rate
27 in both catchments for this event.

28 For the two major drought events the number of intermittent events were no more than 3.
29 These events had not significant impact in the drought pattern.

30

1 From Fig. 6, two small soil water drought events in 2011 were observed for Calluancay and
2 just one event in Cumbe. These dry periods occurred within the wet season and so, the
3 duration is no more than 50 days in both catchments (46 and 13 days for Calluancay and 34
4 days for Cumbe). The recovery rates for those events were equals to 3.03, 8.76 and 5.00 %
5 recovery day⁻¹. The anomalies calculated for those events were different -47.3, -40.6 for
6 Calluancay and -72.1% for Cumbe. The latest event was buffered almost completely by the
7 soil water storage of Cumbe. This is confirmed by Fig. 6, a small hydrological drought event
8 is generated by the anomaly observed in the precipitation. In a similar way, in Calluancay, the
9 second event observed in that period was buffered by the soil water storage and hence, a
10 hydrological drought event was not generated.

11 In 2012, one minor soil water drought event was identified in Calluancay. The anomaly was
12 equal to -44.7%. The drought recovery was reached in 8 days. The recovery rate was equal to
13 8.31% recovery day⁻¹. The duration of the drought was as short as 18 days.

14 **4.6 Vegetation stress and recovery**

15 The vegetation stress periods were identified when the potential evapotranspiration exceeds
16 the precipitation. Monthly data of E_p and P were used in the identification of the vegetation
17 stress periods. As result, for Calluancay the months from August 2009 up to January 2010
18 reveal clearly a deficit of water (Fig. 7a). This was confirmed by the modelling results, E_a was
19 reduced substantially during this period as compared with E_p . In addition, the end of the soil
20 water drought happened in February 2010 (Fig. 6a) and so, the vegetation stress recovery
21 started and the soil water content progressively increased during the wet season. The complete
22 recovery was reached in June 2010 when E_a was 92% of the E_p (maximum value reached in
23 the wet season).

24 Between August and November 2010, another vegetation stress period was identified.. The
25 vegetation stress recovery period was between December 2010 and April 2011 by the onset of
26 the wet season. The maximum monthly value of E_a was equal to 86% of E_p for this recovery
27 period. While, the soil water drought recovery was reached in February 2011. In this month,
28 E_a was equal to 76% of E_p .

29 In 2011, August and October revealed a deficit of water with a quick recovery due to
30 sufficient precipitation during November 2011 and February 2012 (here the maximum
31 monthly E_a was equal to 93% of E_p). While, in 2012 the similar period between July to

1 September suffered a deficit. A partial recovery was observed in October and November
2 2012.

3 Finally, in Cumbe the vegetation stress was higher as compared to Calluancay (Fig.7b). From
4 July 2009 up to January 2010 (7 consecutive months of vegetation stress). For instance, in
5 August 2009 the precipitation recorded in Cumbe was only 6.5 mm, while in Calluancay it
6 was 24.2 mm. In February 2010, the end of the soil water drought recovery was observed and
7 so, this marked the beginning of the vegetation recovery period. The recovery was reached
8 completely on June 2010 and so, E_a was equal to 91% of E_p (but with anomalies in March and
9 April 2010) just before the onset of the second drought period.

10 The second vegetation stress period was identified between August 2010 and January 2011.
11 Intermittent recoveries are observed during February and April 2011. In fact, these months
12 were the end of the soil water drought recovery respectively. The E_a estimated for those
13 months was equal to 74 and 86% of E_p .

14 The third vegetation stress period was observed from August to December 2011. For this
15 event, the recovery period was reached completely in February 2012 (only two months of
16 recovery) and so, the E_a was equal to 86% of E_p . The last vegetation stress period was from
17 March up to November 2012. This marked the end of our monitoring period so we cannot
18 provide an estimation of the complete recovery period.

19 **4.7 Sensitivity analysis**

20 Here, we studied two relatively simple scenarios, in both cases we kept the parameter set
21 obtained during the calibration procedure. This means, the soil characteristics were not
22 modified. Only precipitation and potential evapotranspiration were exchanged between the
23 catchments in order to assess the impact in the soil water storage by means of simulations
24 with the hydrological model.

25 The Fig 8 revealed that the most important factor was the precipitation as compared to the
26 potential evapotranspiration. The stream discharge was drastically reduced during the wet
27 season in April 2012, as consequence of the increase in the deficit of soil water storage. A
28 significant difference was not observed in the drought periods of 2009-2010 or 2011 despite
29 of the increase in the rate of E_p and by a reduction in the input of rain. The opposite occurred
30 in Cumbe, mainly due to the increase in the precipitation amount and by a reduction in the
31 potential evapotranspiration rate. So, the stream discharge was substantially increased along

1 the whole period, as consequence of the reduction of soil water storage deficit. This illustrates
2 the importance whether the rainfall minus potential evapotranspiration shows a surplus or
3 deficit.

4 **4.8 Drought characteristics**

5 The combinations of durations and standardized deficits for the drought events revealed no
6 difference between the catchments. Initially, we can infer that the drought events are
7 independent of the climate. The maximum standardized deficit estimated was no more than 9
8 days. This mean that no more than 9 days with mean flow are required to reduce the deficit to
9 zero (Van Loon et al., 2014). While, the sensitivity analysis revealed that the precipitation is
10 the main factor and has a direct influence over the hydrological response of the catchments,
11 especially during the drought recovery.

12 The soil water drought propagation analysis showed the buffering capacity of the soil water
13 storage. The buffering capacity of the soils was important in the drought of 2010-2011 and
14 partially in the previous event 2009-2010. Comparing the drought analysis for soil water
15 storage and stream discharge clearly showed that they were linked. The seasonality observed
16 in the rainfall climate during the monitoring period is also reflected by the temporal
17 variability of the soil water storage with some delay due to buffering.

18 In the drought event of 2009-2010, the vegetation stress observed in Cumbe lasted seven
19 consecutive months of water deficit as compared to six months of Calluancay. The onset of
20 the drought coincided with the dry season. The vegetation recovery occurred during the wet
21 season in both catchments and when the maximum actual evapotranspiration reached 93% of
22 the potential vegetation evapotranspiration.

23 After the drought event of 2009-2010 in Calluancay and Cumbe, the vegetation recovery was
24 reached in three and five months, respectively. For Calluancay, the three months were
25 consecutive, while in Cumbe the recovery occurred with intermittent periods of stress. In the
26 second drought event 2010-2011, the recovery was equal to five and six months for
27 Calluancay and Cumbe respectively.

28 Finally, point measurements of soil water content in both catchments revealed high
29 differences during drought events (Fig. 4). A faster recovery was observed in páramo as
30 compared to the grasslands of Cumbe. Nevertheless, whether soil water storage simulations -

1 catchment scale- are used instead of plot measurements, the differences in the speed of
2 recovery is no more than a 37% (drought event 2009-2010).

4 **5 Conclusions**

5 The páramo ecosystem has a pivotal role in the hydrology and ecology for the highlands
6 above 3500m in the Andean region. The páramo is the main source of water for human
7 consumption, irrigation and hydropower. Therefore, we compared the hydrological response
8 of a typical catchment on páramo at 3500 m a.s.l. to one with lower grassland at 2600 m a.s.l.
9 during drought events in 2009, 2010, 2011 and 2012. The analysis was carried out based on
10 the calibration and validation of a hydrological conceptual model, the PDM model and
11 compared to soil water measurements in plots.

12 Based on the threshold method the soil moisture droughts occurred mainly in the dry season
13 in both catchments as a consequence of several anomalies in the precipitation (meteorological
14 drought). Just one soil moisture drought was observed during the wet season (in 2011). The
15 deficit for all cases is small and progressively reduced during the wet season. This conclusion
16 is confirmed by the identification of the vegetation stress periods. These periods correspond
17 mainly to the months of September, October and November which coincides with the dry
18 season. In this context, the maximum number of consecutive dry days were reached during
19 the drought of 2009 and 2010, 19 and 22 days, which can be considered a record in páramo.
20 In these periods, the soil moisture content observed in the experimental plot reached also the
21 lowest values recoded until now, $0.60 \text{ cm}^3 \text{ cm}^{-3}$ in November 2009.

22 At the plot scale the differences between the recovery of the soils were relatively large. The
23 measured water content in páramo soils showed a quicker recovery as compared with the
24 mineral soils in Cumbe. But, at the catchment scale, the soil water storage simulated by PDM
25 model and the drought analysis was not as pronounced. Only for the prolonged drought event
26 of 2009-2010 the differences were larger. The main factor in the hydrological response of
27 these experimental catchments is the precipitation relative to potential evapotranspiration. As
28 the soils never became extremely dry or close to wilting point the soil water storage capacity
29 has a secondary influence. The altitude with lower temperatures has a lower water demand for
30 vegetation. The rainfall minus potential vegetation evaporation has therefore more impact as
31 compared to the influence of the soil water storage capacity.

1

2 **Acknowledgements**

3 We thank the VLIR-IUC programme and IFS for its financial support during this research.
4 And also thanks to the anonymous referee and Dr. Wouter Buytaert by their comments in
5 order to improve the present manuscript.

6

7 **References**

- 8 Allen, R., Pereira, L. S., Raes, D. and Smith, M.: Crop evapotranspiration. Guidelines for
9 Computing Crop Water Requirements. FAO Irrigation and Drainage Paper 56. FAO, Rome.,
10 1998.
- 11 Andreadis, K. M., Clark, E. a., Wood, A. W., Hamlet, A. F. and Lettenmaier, D. P.:
12 Twentieth-Century Drought in the Conterminous United States, *Journal of*
13 *Hydrometeorology*, 6(6), 985–1001, doi:10.1175/JHM450.1, 2005.
- 14 Buytaert, W. and Beven, K.: Models as multiple working hypotheses: hydrological simulation
15 of tropical alpine wetlands, *Hydrological Processes*, 25(11), 1784–1799,
16 doi:10.1002/hyp.7936, 2011.
- 17 Buytaert, W. and De Bièvre, B.: Water for cities: The impact of climate change and
18 demographic growth in the tropical Andes, *Water Resources Research*, 48(8), W08503,
19 doi:10.1029/2011WR011755, 2012.
- 20 Buytaert, W., Célleri, R., De Bièvre, B., Cisneros, F., Wyseure, G., Deckers, J. and Hofstede,
21 R.: Human impact on the hydrology of the Andean páramos, *Earth-Science Reviews*, 79(1-2),
22 53–72, doi:10.1016/j.earscirev.2006.06.002, 2006a.
- 23 Buytaert, W., Celleri, R., Willems, P., Bièvre, B. De and Wyseure, G.: Spatial and temporal
24 rainfall variability in mountainous areas: A case study from the south Ecuadorian Andes,
25 *Journal of Hydrology*, 329(3-4), 413–421, doi:10.1016/j.jhydrol.2006.02.031, 2006b.
- 26 Buytaert, W., Cuesta-Camacho, F. and Tobón, C.: Potential impacts of climate change on the
27 environmental services of humid tropical alpine regions, *Global Ecology and Biogeography*,
28 20(1), 19–33, doi:10.1111/j.1466-8238.2010.00585.x, 2011.
- 29 Buytaert, W., Deckers, J. and Wyseure, G.: Regional variability of volcanic ash soils in south
30 Ecuador: The relation with parent material, climate and land use, *Catena*, 70(2), 143–154,
31 doi:10.1016/j.catena.2006.08.003, 2007a.
- 32 Buytaert, W., Iñiguez, V. and Bièvre, B. De: The effects of afforestation and cultivation on
33 water yield in the Andean páramo, *Forest Ecology and Management*, 251(1-2), 22–30,
34 doi:10.1016/j.foreco.2007.06.035, 2007b.
- 35 Buytaert, W., Iñiguez, V., Celleri, R., De Bièvre, B., Wyseure, G. and Deckers, J.: Analysis of
36 the Water Balance of Small Páramo Catchments in South Ecuador, in *Environmental Role of*
37 *Wetlands in Headwaters SE - 24*, vol. 63, edited by J. Krecek and M. Haigh, pp. 271–281,
38 Springer Netherlands, Dordrecht, The Netherlands., 2006c.

- 1 Buytaert, W., Vuille, M., Dewulf, A., Urrutia, R., Karmalkar, A. and Céleri, R.: Uncertainties
2 in climate change projections and regional downscaling in the tropical Andes: implications for
3 water resources management, *Hydrology and Earth System Sciences*, 14(7), 1247–1258,
4 doi:10.5194/hess-14-1247-2010, 2010.
- 5 Buytaert, W., Wyseure, G., De Bièvre, B. and Deckers, J.: The effect of land-use changes on
6 the hydrological behaviour of Histic Andosols in south Ecuador, *Hydrological Processes*,
7 19(20), 3985–3997, doi:10.1002/hyp.5867, 2005.
- 8 Celleri, R., Willems, P., Buytaert, W. and Feyen, J.: Space–time rainfall variability in the
9 Paute basin, Ecuadorian Andes, *Hydrological Processes*, 21(24), 3316–3327,
10 doi:10.1002/hyp.6575, 2007.
- 11 Dai, A.: Drought under global warming: A review, *Wiley Interdisciplinary Reviews: Climate
12 Change*, 2(1), 45–65, doi:10.1002/wcc.81, 2011.
- 13 Dercon, G., Bossuyt, B., De Bièvre, B., Cisneros, F. and Deckers, J.: Zonificación
14 agroecológica del Austro Ecuatoriano, U Ediciones, Cuenca, Ecuador., 1998.
- 15 Dercon, G., Govers, G., Poesen, J., Sánchez, H., Rombaut, K., Vandebroek, E., Loaiza, G.
16 and Deckers, J.: Animal-powered tillage erosion assessment in the southern Andes region of
17 Ecuador, *Geomorphology*, 87(1-2), 4–15, doi:10.1016/j.geomorph.2006.06.045, 2007.
- 18 Duan, Q., Sorooshian, S. and Gupta, V.: Effective and efficient global optimization for
19 conceptual rainfall-runoff models, *Water Resources Research*, 28(4), 1015–1031,
20 doi:10.1029/91WR02985, 1992.
- 21 FAO, ISRIC and ISSS: World Reference Base for Soil Resources. No. 84 in World Soil
22 Resources Reports. FAO, Rome., 1998.
- 23 Farley, K. a., Kelly, E. F. and Hofstede, R. G. M.: Soil Organic Carbon and Water Retention
24 after Conversion of Grasslands to Pine Plantations in the Ecuadorian Andes, *Ecosystems*,
25 7(7), 729–739, doi:10.1007/s10021-004-0047-5, 2004.
- 26 Garcia, M., Raes, D., Allen, R. and Herbas, C.: Dynamics of reference evapotranspiration in
27 the Bolivian highlands (Altiplano), *Agricultural and Forest Meteorology*, 125(1-2), 67–82,
28 doi:10.1016/j.agrformet.2004.03.005, 2004.
- 29 Guzmán, P., Anibas, C., Batelaan, O., Huysmans, M. and Wyseure, G.: Hydrological
30 connectivity of alluvial Andean valleys: a groundwater/surface-water interaction case study in
31 Ecuador, *Hydrogeology Journal*, doi:10.1007/s10040-015-1361-z, 2016.
- 32 Hargreaves, G. H. and Samani, Z. A.: Reference Crop Evapotranspiration from Temperature,
33 *Applied Engineering in Agriculture*, 1(2), 96–99, 1985.
- 34 Hofstede, R. G. M., Groenendijk, J. P., Coppus, R., Fehse, J. C. and Sevink, J.: Impact of Pine
35 Plantations on Soils and Vegetation in the Ecuadorian High Andes, *Mountain Research and
36 Development*, 22(2), 159–167, doi:10.1659/0276-4741(2002)022[0159:IOPPOS]2.0.CO;2,
37 2002.
- 38 Hofstede, R., Segarra, P. and Mena, P.: Los páramos del mundo, *Global Peatland
39 Initiative/NC-IUCN/EcoCiencia*, Quito., 2003.
- 40 Hungerbühler, D., Steinmann, M., Winkler, W., Seward, D., Egüez, A., Peterson, D. E., Helg,
41 U. and Hammer, C.: Neogene stratigraphy and Andean geodynamics of southern Ecuador,
42 *Earth-Science Reviews*, 57(1-2), 75–124, doi:10.1016/S0012-8252(01)00071-X, 2002.

- 1 Kilpatrick, F. and Schneider, V.: Use of flumes in measuring discharge, U.S. Geological
2 Survey Techniques of Water Resources Investigations, Washington, USA., 1983.
- 3 Kim, T.-W., Valdés, J. B. and Yoo, C.: Nonparametric Approach for Estimating Return
4 Periods of Droughts in Arid Regions, *Journal of Hydrologic Engineering*, 8(5), 237–246,
5 doi:10.1061/(ASCE)1084-0699(2003)8:5(237), 2003.
- 6 Klemeš, V.: Operational testing of hydrological simulation models, *Hydrological Sciences*
7 *Journal*, 31(1), 13–24, doi:10.1080/02626668609491024, 1986.
- 8 Koch, K., Wenninger, J., Uhlenbrook, S. and Bonell, M.: Joint interpretation of hydrological
9 and geophysical data: electrical resistivity tomography results from a process hydrological
10 research site in the Black Forest Mountains, Germany, *Hydrological Processes*, 23(10), 1501–
11 1513, doi:10.1002/hyp.7275, 2009.
- 12 Liefvendahl, M. and Stocki, R.: A study on algorithms for optimization of Latin hypercubes,
13 *Journal of Statistical Planning and Inference*, 136(9), 3231–3247,
14 doi:10.1016/j.jspi.2005.01.007, 2006.
- 15 Lloyd-Hughes, B. and Saunders, M. A.: A drought climatology for Europe, *International*
16 *Journal of Climatology*, 22(13), 1571–1592, doi:10.1002/joc.846, 2002.
- 17 Luteyn, J. L.: *Páramos: A Checklist of Plant Diversity, Geographical Distribution, and*
18 *Botanical Literature*. The New York Botanical Garden Press, New York., 1999.
- 19 Moore, R. J.: The probability-distributed principle and runoff production at point and basin
20 scales, *Hydrological Sciences Journal*, 30(2), 273–297, doi:10.1080/02626668509490989,
21 1985.
- 22 Moore, R. J. and Clarke, R. T.: A distribution function approach to rainfall runoff modeling,
23 *Water Resources Research*, 17(5), 1367–1382, doi:10.1029/WR017i005p01367, 1981.
- 24 Mora, D. E., Campozano, L., Cisneros, F., Wyseure, G. and Willems, P.: Climate changes of
25 hydrometeorological and hydrological extremes in the Paute basin, Ecuadorian Andes,
26 *Hydrology and Earth System Sciences*, 18(2), 631–648, doi:10.5194/hess-18-631-2014, 2014.
- 27 Nash, J. E. and Sutcliffe, J. V.: River flow forecasting through conceptual models part I — A
28 discussion of principles, *Journal of Hydrology*, 10(3), 282–290, doi:10.1016/0022-
29 1694(70)90255-6, 1970.
- 30 Parry, S., Wilby, R. L., Prudhomme, C. and Wood, P. J.: A systematic assessment of drought
31 termination in the United Kingdom, *Hydrology and Earth System Sciences Discussions*,
32 (January), 1–33, doi:10.5194/hess-2015-476, 2016.
- 33 Pebesma, E. J.: Multivariable geostatistics in S: the gstat package, *Computers & Geosciences*,
34 30(7), 683–691, doi:10.1016/j.cageo.2004.03.012, 2004.
- 35 Peters, E., Bier, G., van Lanen, H. A. J. and Torfs, P. J. J. F.: Propagation and spatial
36 distribution of drought in a groundwater catchment, *Journal of Hydrology*, 321(1-4), 257–
37 275, doi:10.1016/j.jhydrol.2005.08.004, 2006.
- 38 Podwojewski, P., Poulénard, J., Zambrana, T. and Hofstede, R.: Overgrazing effects on
39 vegetation cover and properties of volcanic ash soil in the páramo of Llangahua and La
40 Esperanza (Tungurahua, Ecuador), *Soil Use and Management*, 18, 45–55, doi:10.1111/j.1475-
41 2743.2002.tb00049.x, 2002.
- 42 Ramsay, P. M. and Oxley, E. R. B.: The growth form composition of plant communities in

1 the ecuadorian páramos, *Plant Ecology*, 131(2), 173–192, doi:10.1023/A:1009796224479,
2 1997.

3 Romano, N.: Soil moisture at local scale: Measurements and simulations, *Journal of*
4 *Hydrology*, 516, 6–20, doi:10.1016/j.jhydrol.2014.01.026, 2014.

5 Schneider, P., Vogt, T., Schirmer, M., Doetsch, J., Linde, N., Pasquale, N., Perona, P. and
6 Cirpka, O. a.: Towards improved instrumentation for assessing river-groundwater interactions
7 in a restored river corridor, *Hydrology and Earth System Sciences*, 15(8), 2531–2549,
8 doi:10.5194/hess-15-2531-2011, 2011.

9 Southgate, D. and Macke, R.: The Downstream Benefits of Soil Conservation in Third World
10 Hydroelectric Watersheds, *Land Economics*, 65(1), 38, doi:10.2307/3146262, 1989.

11 Stocki, R.: A method to improve design reliability using optimal Latin hypercube sampling,
12 *Computer Assisted Mechanics and Engineering Sciences*, (12), 393–411, 2005.

13 Tsakiris, G., Nalbantis, I., Vangelis, H., Verbeiren, B., Huysmans, M., Tychon, B.,
14 Jacquemin, I., Canters, F., Vanderhaegen, S., Engelen, G., Poelmans, L., De Becker, P. and
15 Batelaan, O.: A System-based Paradigm of Drought Analysis for Operational Management,
16 *Water Resources Management*, 27(15), 5281–5297, doi:10.1007/s11269-013-0471-4, 2013.

17 Vanacker, V., Molina, A., Govers, G., Poesen, J. and Deckers, J.: Spatial variation of
18 suspended sediment concentrations in a tropical Andean river system: The Paute River,
19 southern Ecuador, *Geomorphology*, 87(1-2), 53–67, doi:10.1016/j.geomorph.2006.06.042,
20 2007.

21 van Genuchten, M. T.: A Closed-form Equation for Predicting the Hydraulic Conductivity of
22 Unsaturated Soils, *Soil Science Society of America Journal*, 44, 892–898,
23 doi:10.2136/sssaj1980.03615995004400050002x, 1980.

24 Van Lanen, H. A. J., Wanders, N., Tallaksen, L. M. and Van Loon, A. F.: Hydrological
25 drought across the world: impact of climate and physical catchment structure, *Hydrology and*
26 *Earth System Sciences*, 17(5), 1715–1732, doi:10.5194/hess-17-1715-2013, 2013.

27 Van Loon, a. F., Tjeldeman, E., Wanders, N., Van Lanen, H. A. J., Teuling, a. J. and
28 Uijlenhoet, R.: How climate seasonality modifies drought duration and deficit, *Journal of*
29 *Geophysical Research: Atmospheres*, 119(8), 4640–4656, doi:10.1002/2013JD020383, 2014.

30 Van Loon, A. F.: On the propagation of drought. How climate and catchment characteristics
31 influence hydrological drought development and recovery, PhD Thesis, Wageningen
32 University, Wageningen, the Netherlands., 2013.

33 Van Loon, A. F.: Hydrological drought explained, *Wiley Interdisciplinary Reviews: Water*,
34 2(4), 359–392, doi:10.1002/wat2.1085, 2015.

35 Vicente-Serrano, S. M., Gouveia, C., Camarero, J. J., Beguería, S., Trigo, R., López-Moreno,
36 J. I., Azorín-Molina, C., Pasho, E., Lorenzo-Lacruz, J., Revuelto, J., Morán-Tejeda, E. and
37 Sanchez-Lorenzo, A.: Response of vegetation to drought time-scales across global land
38 biomes., *Proceedings of the National Academy of Sciences of the United States of America*,
39 110(1), 52–7, doi:10.1073/pnas.1207068110, 2013.

40 Viviroli, D., Archer, D. R., Buytaert, W., Fowler, H. J., Greenwood, G. B., Hamlet, a. F.,
41 Huang, Y., Koboltschnig, G., Litaor, M. I., López-Moreno, J. I., Lorentz, S., Schädler, B.,
42 Schreier, H., Schwaiger, K., Vuille, M. and Woods, R.: Climate change and mountain water
43 resources: overview and recommendations for research, management and policy, *Hydrology*

1 and Earth System Sciences, 15(2), 471–504, doi:10.5194/hess-15-471-2011, 2011.
2 Wagener, T., Boyle, D. P., Lees, M. J., Wheater, H. S., Gupta, H. V. and Sorooshian, S.: A
3 framework for development and application of hydrological models, Hydrology and Earth
4 System Sciences, 5(1), 13–26, doi:10.5194/hess-5-13-2001, 2001.
5 Wanders, N., van Lanen, H. A. J. and van Loon, A. F.: Indicators for drought characterization
6 on a global scale, WATCH Technical Report No. 24. [online] Available from: [www.eu-
7 watch.org/publications/technical-reports](http://www.eu-watch.org/publications/technical-reports), 2010.

8
9
10
11
12
13
14
15
16
17
18
19
20
21
22
23
24
25
26
27

1

2 **Table 1.** The main characteristics of the experimental catchments

Name	Calluancay	Cumbe
Area [km ²]	4.39	44.0
Altitude [m a.s.l.]	3589 - 3882	2647 - 3467
Observation period	Nov 2007 – Nov 2012	Apr 2009 – Nov 2012
Hydrometeorological variables:		
P [mm year ⁻¹]	1095	783
E_p [mm year ⁻¹]	831	1100
Q [mm year ⁻¹]	619	181
-State variables:		
Soil water content [cm ³ cm ⁻³] ^a	0.60 – 0.86	0.39 – 0.54

3 ^a, the average daily minimum and maximum soil water contents for each observation period

4

5

6 **Table 2.** The calibrated parameters of the PDM model.

Parameters	Description	Feasible range	Calluancay	Cumbe
c_{\max}	Maximum storage capacity	30-75 [mm]	64.8	54.5
b	Spatial variability of the storage capacity	0.1-2.0 [-]	0.74	0.17
f_{rt}	Fast routing store residence time	1-2 [days]	1.5	1.4
s_{rt}	Slow routing store residence time	35-120 [days]	58.3	98.2
$\%(q)$	Percentage fast flow	0.25-0.75 [-]	0.51	0.41

7

8

9

10 **Table 3.** The Nash and Sutcliffe efficiencies for the PDM models*.

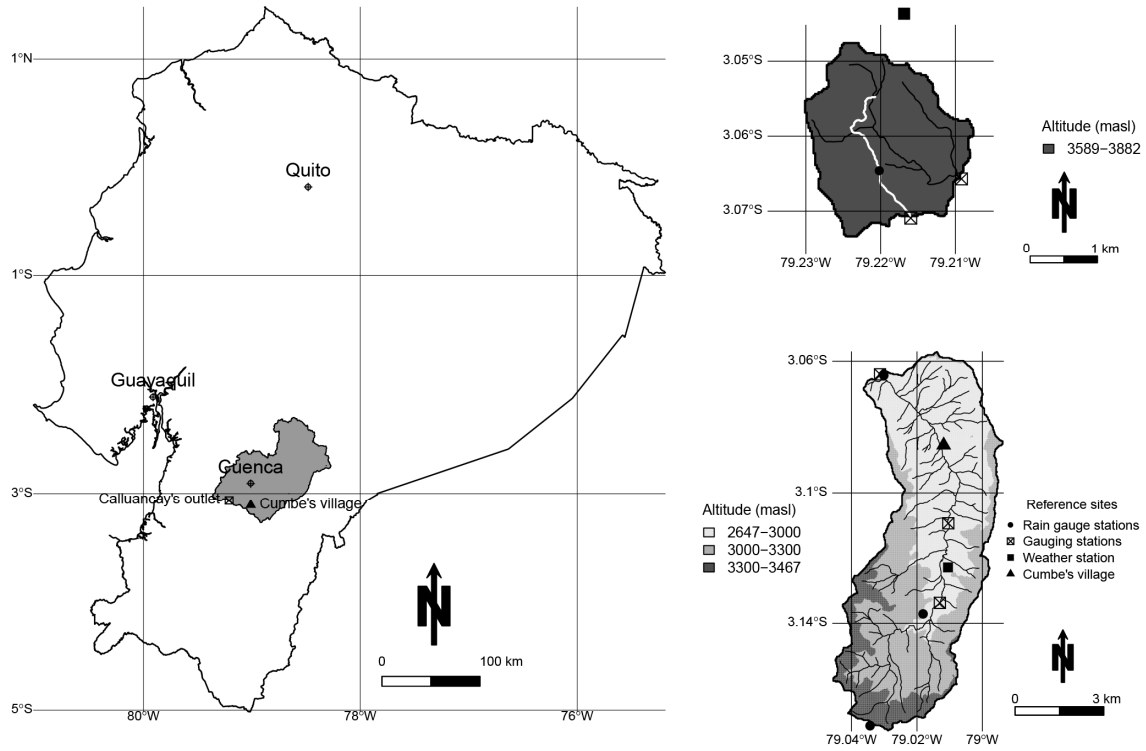
Catchment	Calibration		Validation	
	NS (-)	Period	NS (-)	Period
Calluancay	0.83	29 Nov 2007 – 06 Ago 2009	0.53	20 May 2010 – 27 Nov 2012
Cumbe	0.84	21 Apr 2009 – 17 Apr 2011	0.63	18 Apr 2011 – 13 Dec 2012

11

12 *NS is the Nash and Sutcliffe efficiency based on the logarithms of stream discharges

13

1 **Figure 1.** The study area



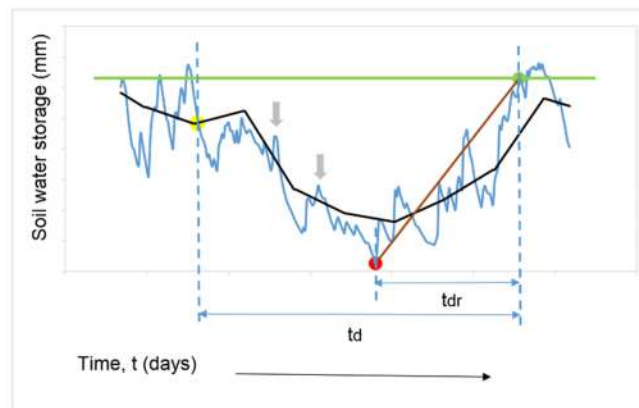
2

3

4

5 **Figure 2.** Conceptual diagram for estimation of the soil moisture drought recovery metrics.

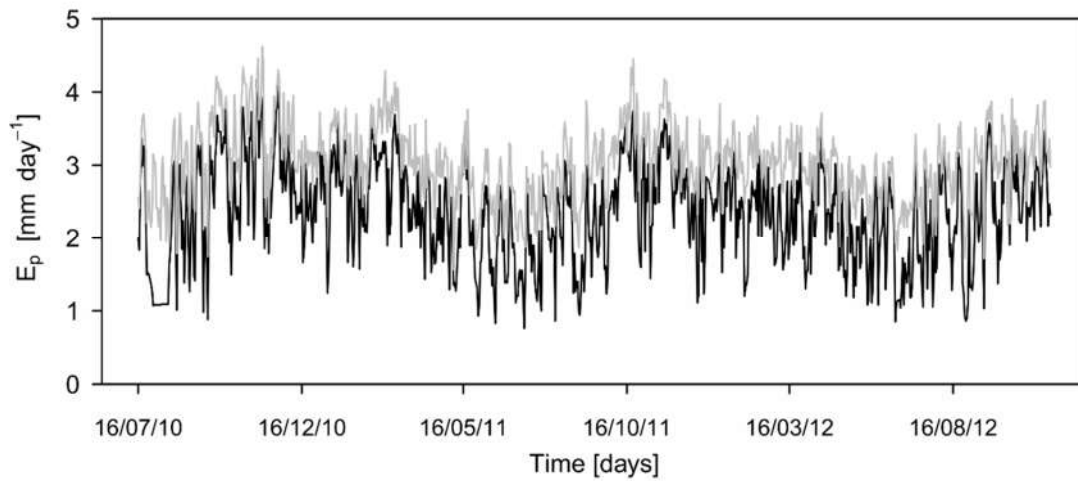
6 The t_d and t_{dr} are the durations in days of the soil moisture drought event and drought recovery period
7 respectively. Drought recovery is represented by a brown line. Grey arrows mark intermittent events above the
8 threshold. Green line marks the assumed normal value of soil water storage.



9

10

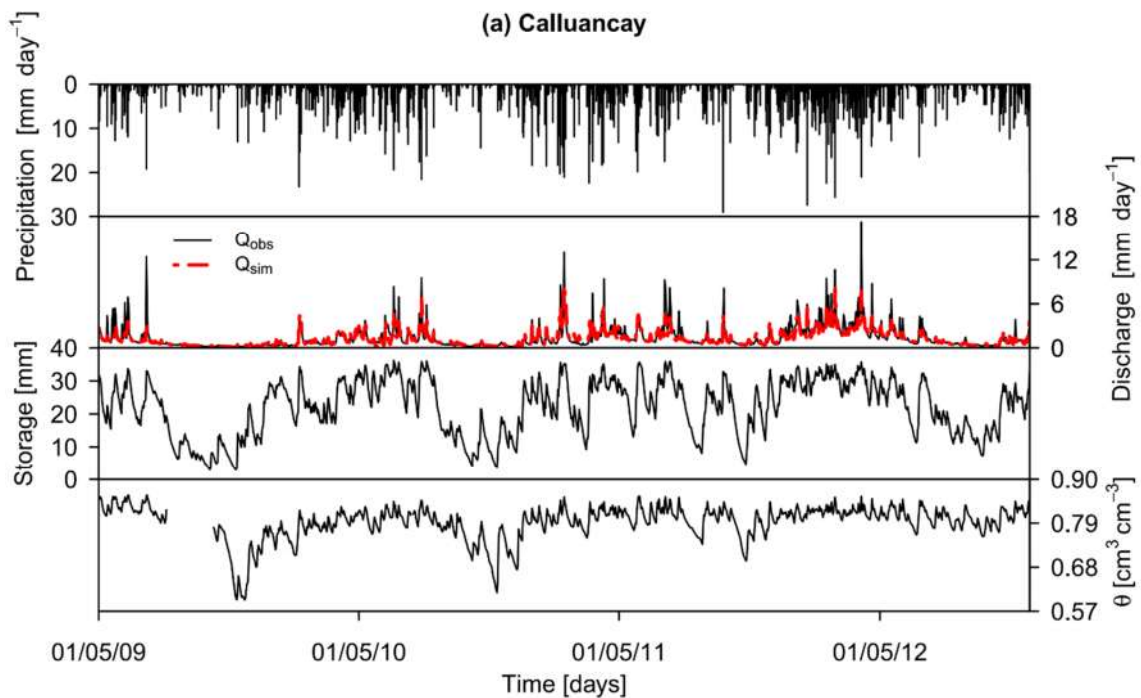
1 **Figure 3.** The potential evapotranspiration E_p for Calluancay (black) and Cumbe (grey).



2

3

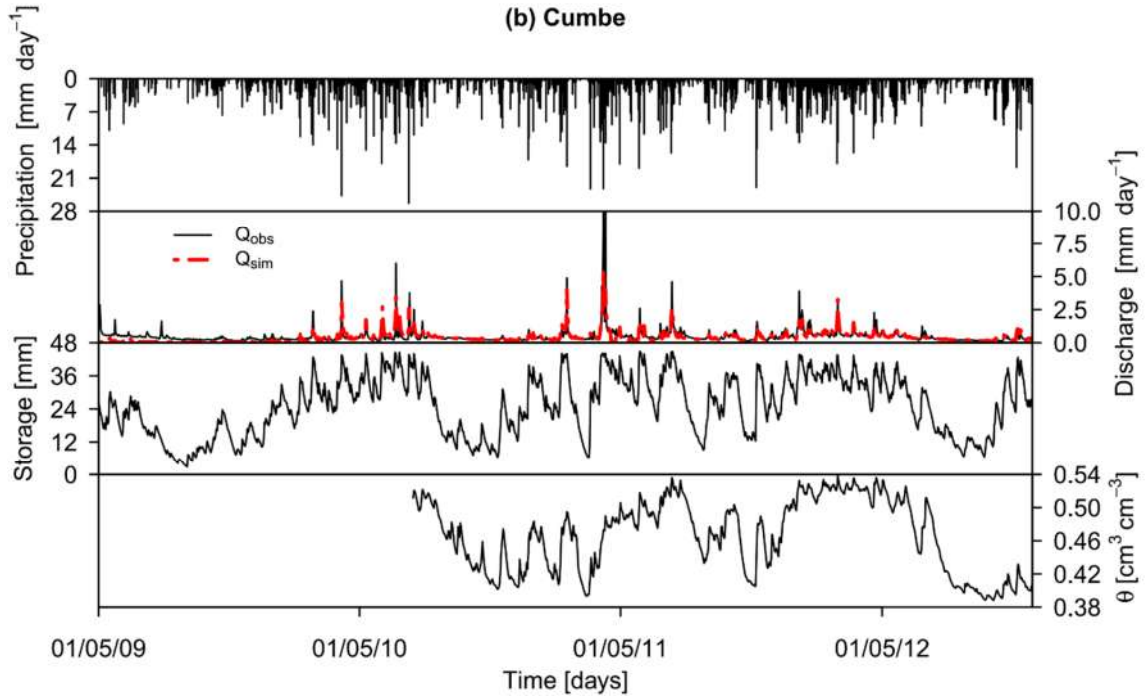
4 **Figure 4.** Results from the hydrological modelling with PDM model. In first panel the
5 precipitation. In the second panel stream discharge observed and simulated Q_{obs} and Q_{sim}
6 respectively. In the third panel the average soil water storage simulated. Finally, in the bottom
7 inset of the plot, the soil moisture measured in an experimental plot.



8

9

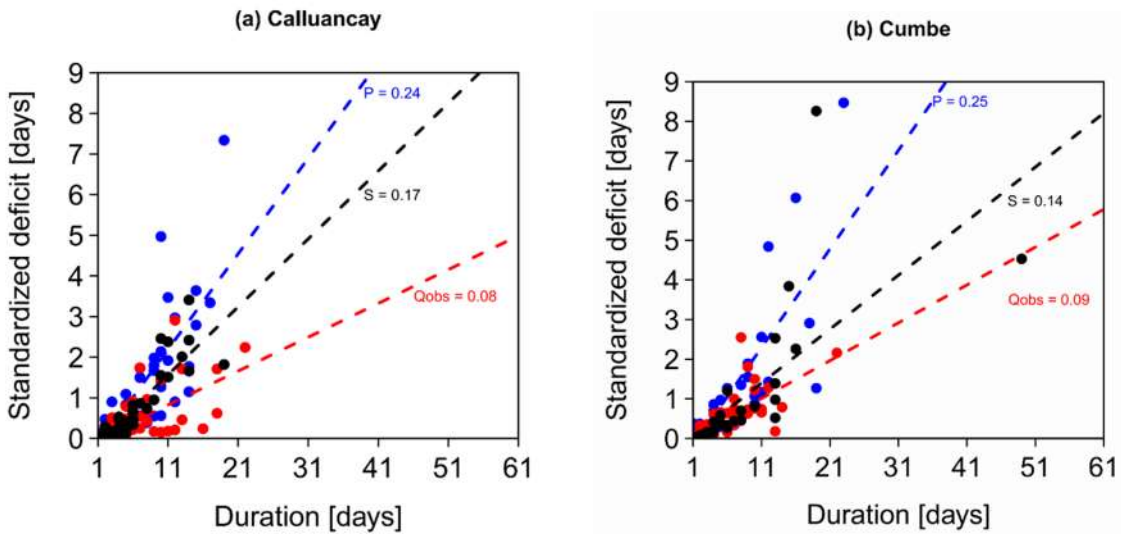
1



2

3

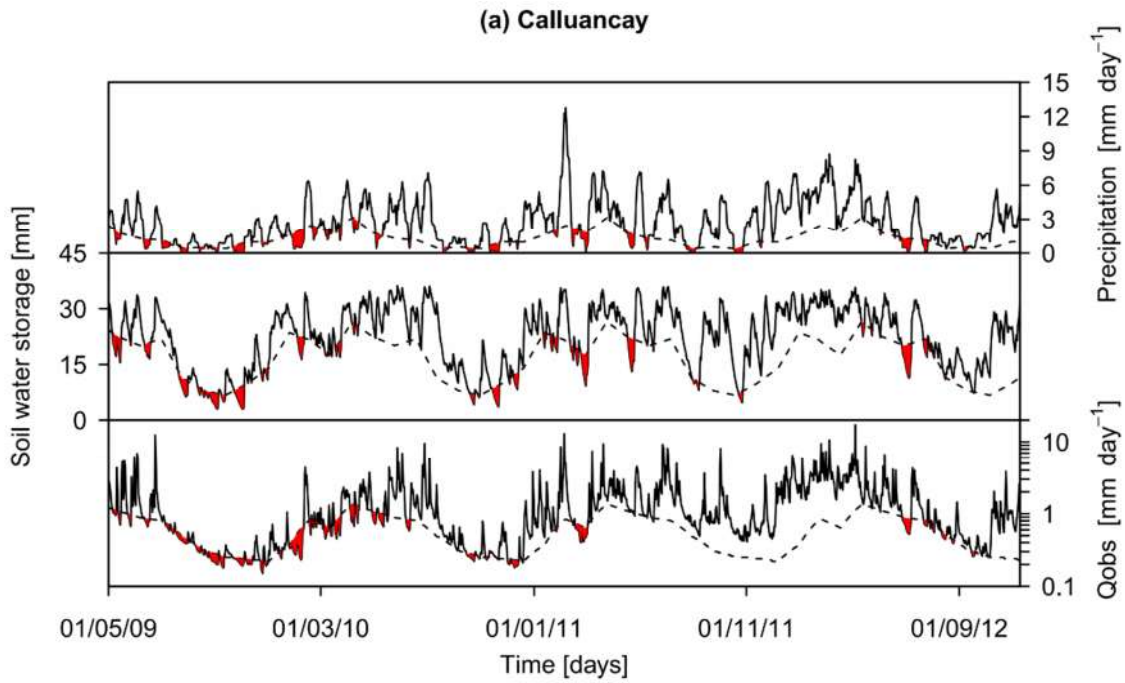
4 **Figure 5.** Standardized deficit for the drought periods. (a) Calluancay and (b) Cumbe (in blue
 5 P, precipitation; in grey S, soil water storage simulated and in orange Q, stream discharge
 6 observed).



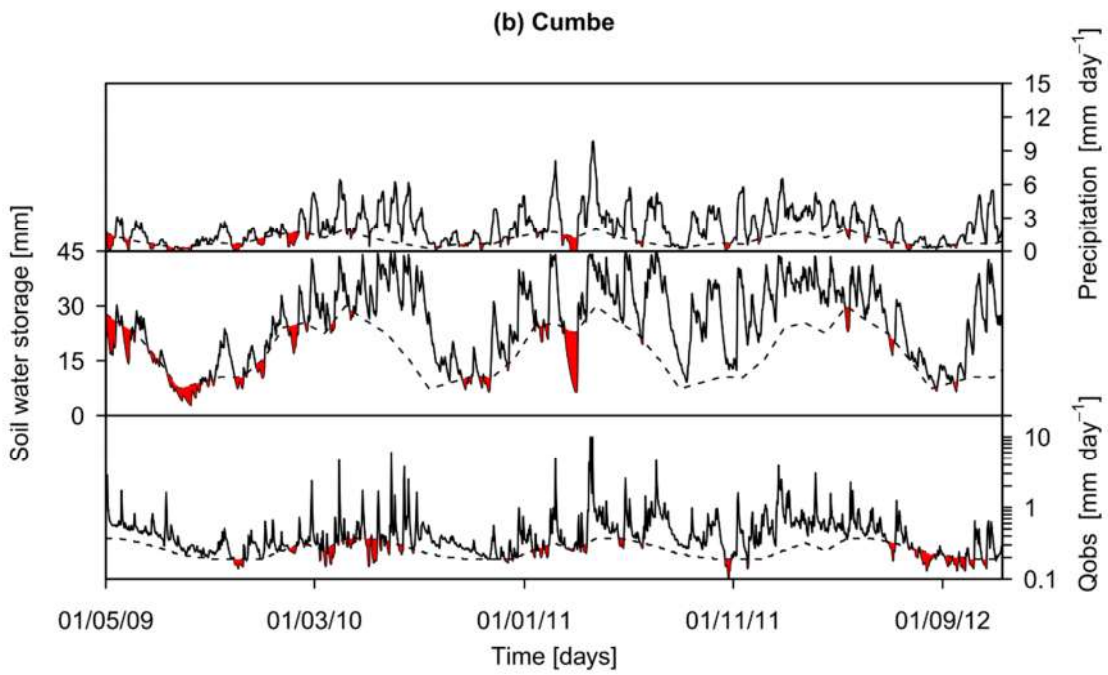
7

8

1 **Figure 6.** Drought propagation for each experimental catchment. Discharge corresponds to
2 the observed data. Soil water storage is the storage simulated by PDM model.

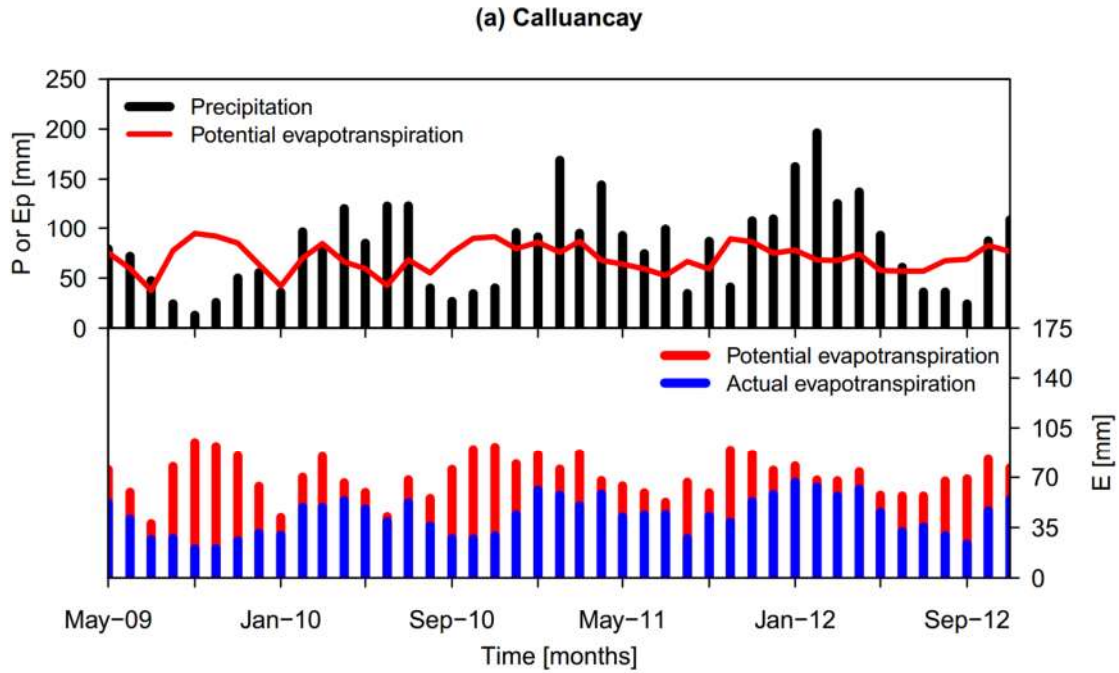


3
4
5



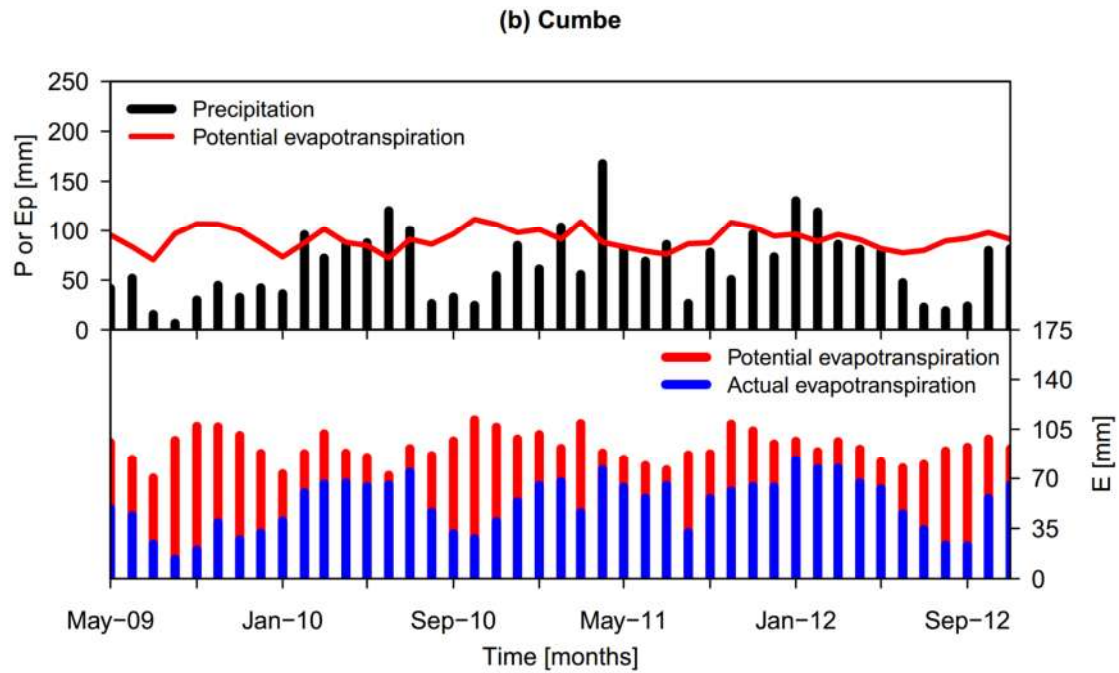
6

1 **Figure 7.** Time series of P , E_p and E_a in order to identify vegetation stress and recovery
 2 periods



3

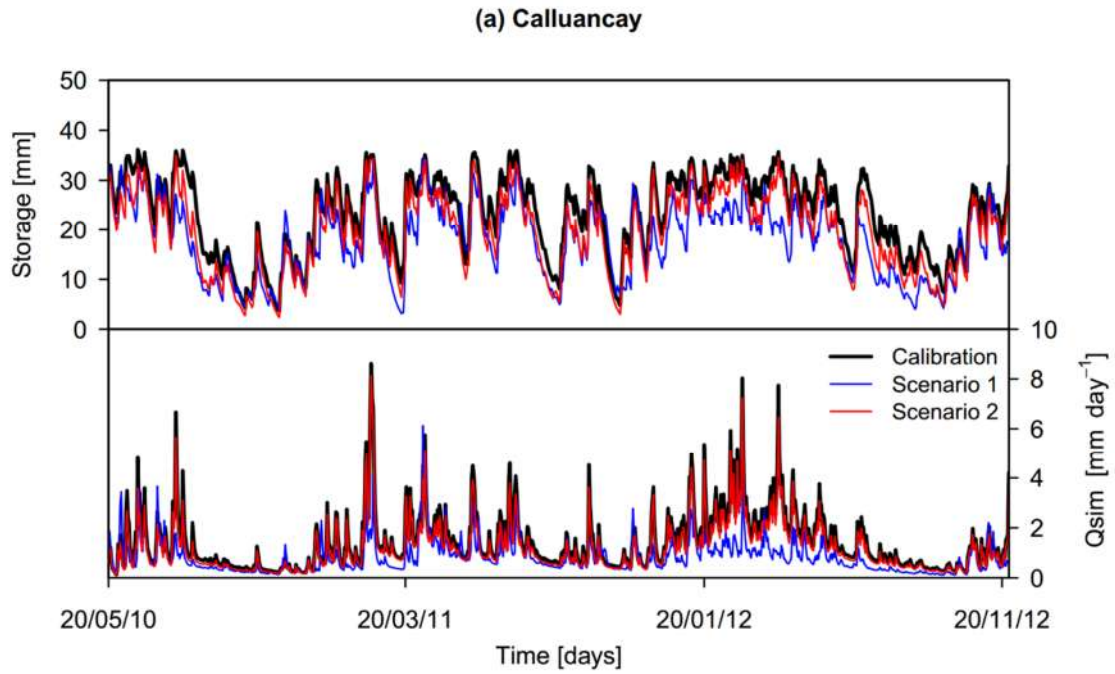
4



5

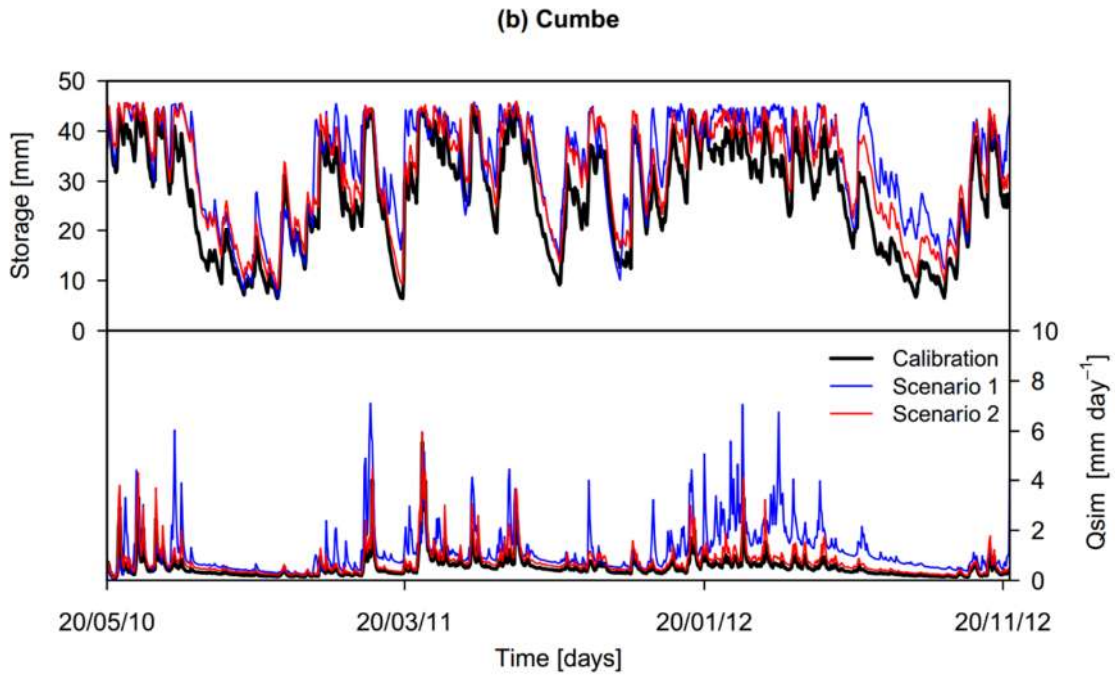
6

1 **Figure 8.** Soil water storage and stream discharge for the experimental catchments as result of
2 the two scenarios of climate. The simulated time series of storage and stream discharge
3 (calibration) are included in the figure for comparison.



4

5



6